

Dihedral F-Tilings of the Sphere by Equilateral and Scalene Triangles-I

A. M. d'AZEVEDO BRED A(*) - PATRÍCIA S. RIBEIRO(**)
ALTINO F. SANTOS(***)

ABSTRACT - The study of dihedral f-tilings of the Euclidean sphere S^2 by triangles and r -sided regular polygons was initiated in 2004 where the case $r = 4$ was considered [6]. In a subsequent paper [1], the study of all spherical f-tilings by triangles and r -sided regular polygons, for any $r \geq 5$, was described. Later on, in [3] the classification of all f-tilings of S^2 whose prototiles are an equilateral triangle (a 3-sided regular polygon) and an isosceles triangle are obtained. In this paper we extend these results presenting the study of all spherical f-tilings by equilateral triangles and scalene triangles in a particular way of adjacency. For this particular case of adjacency, we get two continuous families of f-tilings denoted by \mathcal{F}_1^δ and \mathcal{F}_2^δ . The combinatorial structure including the transitive properties under the action of their symmetry groups is given in Table 1.

1. Introduction

Spherical folding tilings or *f-tilings* for short, are edge-to-edge decompositions of the sphere by geodesic polygons, such that all vertices are of even valency and the sums of alternate angles around each vertex are π , i.e., each vertex is of even valency $2n$, $n \geq 2$ and the sums of alternate

(*) Indirizzo dell'A.: Department of Mathematics, University of Aveiro, 3810-193 Aveiro, Portugal.

E-mail: ambreda@mat.ua.pt

(**) Indirizzo dell'A.: Department of Mathematics, E.S.T. Setúbal, 2910-761, Setúbal, Portugal.

E-mail: pribeiro@est.ips.pt

(***) Indirizzo dell'A.: Department of Mathematics, U.T.A.D., 5001-801, Vila Real, Portugal.

E-mail: afolgado@utad.pt

2000 *Mathematics Subject Classification*: 52C20, 52B05, 20B35.

angles are equal, that is

$$\sum_{i=1}^n \alpha_{2i} = \sum_{i=1}^n \alpha_{2i-1} = \pi,$$

where the angles α_i around any vertex are ordered cyclically. A f-tiling τ is said to be *monohedral* if it is composed by congruent cells, and *dihedral* if every tile of τ is congruent to one of two fixed sets X and Y (prototiles of τ). We shall denote by $\Omega(X, Y)$ the set, up to isomorphism, of all dihedral f-tilings of S^2 whose prototiles are X and Y .

Spherical f-tilings are strongly related to the theory of isometric foldings [9]. The study of this special class of tilings was initiated in [2] with a complete classification of all spherical monohedral f-tilings. The classification of all spherical dihedral folding tilings by rhombi and triangles was recently obtained in 2005, [7].

Here, our interest is focused in spherical triangular dihedral f-tilings whose prototiles are an equilateral triangle and a scalene triangle, in a particular way of adjacency (see I in Figure 1). We end up with two continuous families of f-tilings, illustrated in Figures 18 and 19. The other two cases of adjacency were studied in [4] and [5]. With this study the classification of the spherical f-tilings by two triangular tiles one of which equilateral is now completed.

From now on T_1 denotes an equilateral spherical triangle of angle α and side a and T_2 a scalene spherical triangle of angles δ, γ, β , with the order relation $\delta < \gamma < \beta$ and with sides b (opposite to β), c (opposite to γ) and d (opposite to δ).

We begin by pointing out that any element of $\Omega(T_1, T_2)$ has at least two cells congruent, respectively, to T_1 and T_2 , such that they are in adjacent positions in one and only one of the situations illustrated in Figure 1.

The type I edge-adjacency condition can be analytically described by the equation (see [8])

$$(1.1) \quad \frac{\cos \alpha(1 + \cos \alpha)}{\sin^2 \alpha} = \frac{\cos \beta + \cos \delta \cos \gamma}{\sin \delta \sin \gamma}.$$

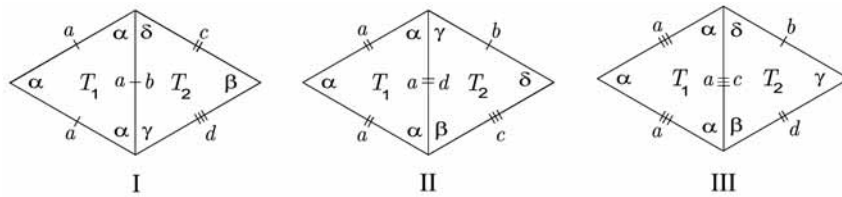


Fig. 1. – Distinct cases of adjacency.

In order to get any dihedral f-tiling $\tau \in \Omega(T_1, T_2)$, we find useful to start by considering one of its *planar representations*, beginning with a common vertex to an equilateral triangle and a scalene triangle in adjacent positions. In the diagrams that follows it is convenient to label the tiles according to the following procedures:

- (i) The tiles by which we begin the planar representation of a tiling $\tau \in \Omega(T_1, T_2)$ are labelled by 1 and 2, respectively;
- (ii) For $j \geq 2$, the location of tile j can be deduced from the configuration of tiles $(1, 2, \dots, j-1)$ and from the hypothesis that the configuration is part of a complete planar representation of a f-tiling (except in the cases indicated).

2. Triangular Dihedral F-Tilings with Adjacency of Type I.

Let T_1 and T_2 be tiles with adjacency of type I.

Starting a planar representation of a such tiling $\tau \in \Omega(T_1, T_2)$ we are led to the one illustrated in Figure 2, where $x \in \{\beta, \gamma\}$.

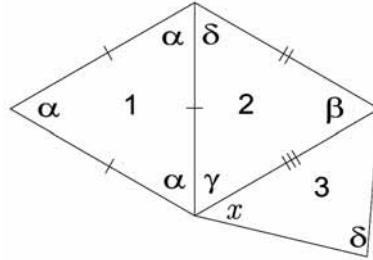


Fig. 2. – Planar representation.

The cases $x = \beta$ and $x = \gamma$ will be studied separately.

Let us begin by assuming that $x = \beta$. Accordingly, $\alpha + \beta \leq \pi$.

PROPOSITION 2.1. *If T_1 and T_2 are tiles with adjacency of type I and $\alpha + x \leq \pi$, with $x = \beta$, then $\Omega(T_1, T_2) = \emptyset$.*

PROOF. Suppose that $\alpha + x = \pi$, with $x = \beta$. The configuration of τ illustrated in Figure 2 expands to the following one (Figure 3).

Since $\alpha + \beta = \gamma + \delta = \pi$ and $\beta > \gamma$, then $\alpha < \delta$. Therefore, $\alpha < \delta < \frac{\pi}{2} < \gamma < \beta$. Accordingly, $\cos \alpha, \cos \delta > 0$ while $\cos \beta, \cos \gamma < 0$ contradicting the adjacency condition 1.1.

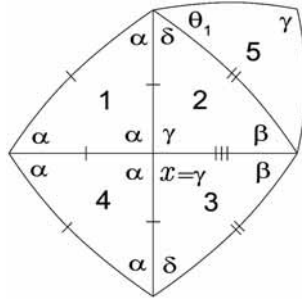


Fig. 5. – Planar representation.

PROPOSITION 2.2. *If T_1 and T_2 are tiles with adjacency of type I and $\alpha + \gamma \leq \pi$, then $\Omega(T_1, T_2) \neq \emptyset$ if and only if $\beta = \frac{\pi}{2}$ and $\alpha + \gamma + \delta = \pi$ ending up with two non isomorphic dihedral f-tilings.*

PROOF. **A)** If $\alpha + \gamma = \pi$, the configuration in Figure 2 expands to the one illustrated in Figure 5.

A decision about the angle $\theta_1 \in \{\delta, \beta\}$ must be taken. Having in account that $\pi = \alpha + \gamma < \alpha + \beta$, then $\theta_1 = \delta$ (Figure 6).

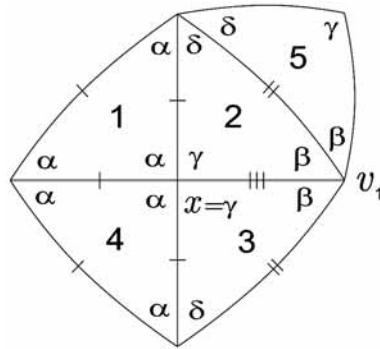


Fig. 6. – Planar representation.

One of the alternate angle sum at vertex v_1 is $2\beta \leq \pi$. If $\beta < \frac{\pi}{2}$ one has $\delta < \gamma < \frac{\pi}{2}$ and $\alpha > \frac{\pi}{2}$, violating the adjacency condition 1.1. Accordingly $\beta = \frac{\pi}{2}$.

B) Consider now that $\alpha + \gamma < \pi$. The angle θ_2 belongs to the set $\{\delta, \beta\}$, see Figure 7.

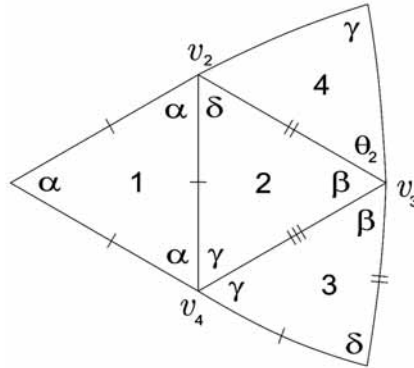


Fig. 7. – Planar representation.

1. Suppose, firstly, that $\theta_2 = \delta$.

The alternate angle sum at vertex v_2 containing α and β satisfies $\alpha + \beta < \pi$, otherwise it would become $\alpha + \beta = \pi = \delta + \gamma$. Therefore, we would have $\alpha < \delta < \frac{\pi}{2} < \gamma < \beta$, not satisfying the adjacency condition 1.1. As $\alpha + \beta < \pi$ and having in account that $\alpha, \beta > \frac{\pi}{3}$ and $\alpha + \beta + \gamma > \pi$ then $\alpha + \beta + k\delta = \pi$, for some $k \geq 1$ (vertex v_2). Now the alternate angle sum containing β and δ at vertex v_3 satisfies $\beta + \delta < \pi$. Summarizing, since $\beta + \gamma + \delta > \pi$ and $\alpha + \beta + k\delta = \pi, k \geq 1$, then $\delta < \frac{\pi}{3} < \alpha < \gamma < \beta$.

Consequently, the alternate angle sum, at vertex v_4 , containing α and γ is $\alpha + \gamma + t\delta = \pi$, for some $t > k \geq 1$. The configuration extends to the one in Figure 8.

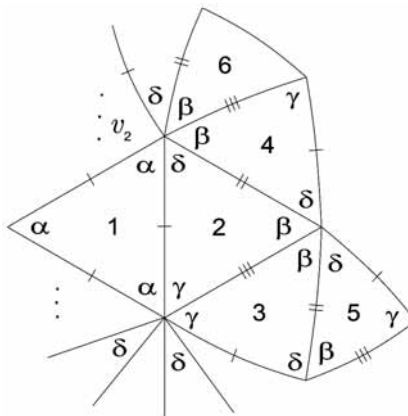


Fig. 8. – Planar representation.

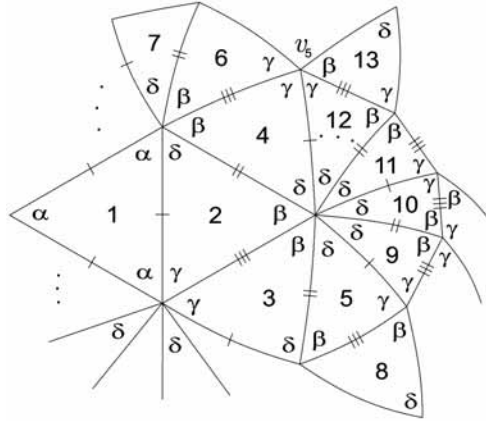


Fig. 11. – Planar representation.

1.2 If $\theta_3 = \gamma$, the configuration in Figure 10 gives rise to the one in Figure 12.

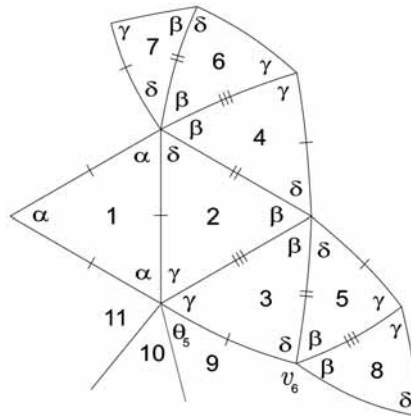


Fig. 12. – Planar representation.

Now, θ_5 is different from δ , otherwise, at vertex v_6 we get the cyclic sequence $(\gamma, \delta, \beta, \beta)$ and the alternate angle sums would be $\beta + \gamma = \pi = \beta + \delta$, which is an absurd. Due to the compatibility of sides in tiles 10 and 11, θ_5 must be different from γ . Therefore, $\theta_5 = \alpha$ and extending the previous configuration, we conclude that $\beta = \frac{\pi}{2}$, see Figure 13.

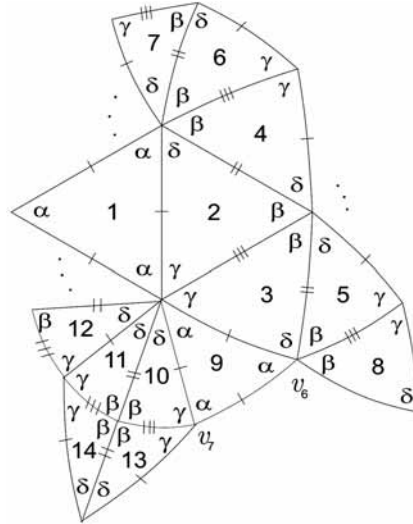


Fig. 13. – Planar representation.

Consequently $\gamma + \delta > \frac{\pi}{2}$ and $\gamma < \frac{\pi}{2}$. Accordingly, $\delta < \frac{\pi}{3} < \alpha < \gamma < \frac{\pi}{2} = \beta$ and all the alternate angle sums containing two angles γ are $2\gamma + \delta = \pi$. Having in account that, $\beta = \frac{\pi}{2}$, $2\gamma + \delta = \pi$, $\alpha + \gamma + t\delta = \pi$ and $\alpha + \beta + k\delta = \pi$, one has $\alpha + k\delta = \frac{\pi}{2}$ and $(1 - 2t - 2k)\delta = 0$, which is absurd since $t > k \geq 1$.

2. Suppose now that $\theta_2 = \beta$ (see Figure 7). Then, $\beta = \frac{\pi}{2}$ and $\alpha < \frac{\pi}{2}$ (otherwise the adjacency condition 1.1 is violated, since $\delta < \gamma < \frac{\pi}{2}$). Also

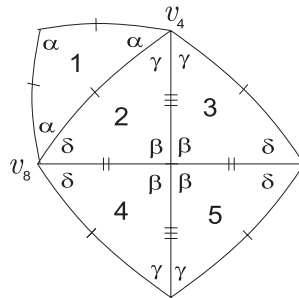


Fig. 14. – Planar representation.

$\delta < \alpha$, otherwise $\delta > \frac{\pi}{3}$ and $\alpha + \delta + \rho > \pi$, for any $\rho \in \{\alpha, \delta, \gamma, \beta\}$. Looking at vertex v_4 in Figure 7, the alternate angle sum containing α and γ is $\alpha + \gamma + \alpha = \pi$ or $\alpha + \gamma + \gamma = \pi$ or $\alpha + \gamma + t\delta = \pi$, for some $t \geq 1$, see Figure 14.

2.1 If $\alpha + \gamma + \alpha = \pi$, then $\frac{\pi}{6} < \delta < \gamma < \frac{\pi}{3} < \alpha$. At vertex v_8 , the alternate angle sum containing α and δ must be

$$2\alpha + \delta = \pi \quad \text{or} \quad \alpha + \delta + \gamma = \pi \quad \text{or} \quad \alpha + 2\delta + \gamma = \pi \quad \text{or} \quad \alpha + 3\delta = \pi.$$

Clearly, the first two cases are impossible. Therefore, $\alpha + 2\delta + \gamma = \pi$ or $\alpha + 3\delta = \pi$. As $\delta + \gamma > \frac{\pi}{2}$ and $\alpha > \gamma$, then $\alpha + 2\delta + \gamma > \pi$ and so $\alpha + 3\delta = \pi$, that is $\delta < \frac{2\pi}{9}$. The angular sequence around vertex v_8 of valency 8, is of the form $(\alpha, \alpha, \delta, \dots, \delta)$ or $(\alpha, \delta, \delta, \alpha, \delta, \dots)$.

Either way, in the expanded configuration, having in account the edge compatibility we get a vertex surrounded by an angular sequence containing four consecutive γ angles, as illustrated in Figure 15. As $\gamma + \delta > \frac{\pi}{2}$ and $\delta < \gamma < \alpha$ then, $2\gamma + \delta < 2\gamma + \gamma < \pi$, $2\gamma + 2\gamma > 2\gamma + 2\delta > \pi$, $2\gamma + \alpha < \gamma + 2\alpha = \pi$ and $3\gamma + \alpha > 3\gamma + \gamma > \pi$. Consequently it is impossible to continue extending the configuration.

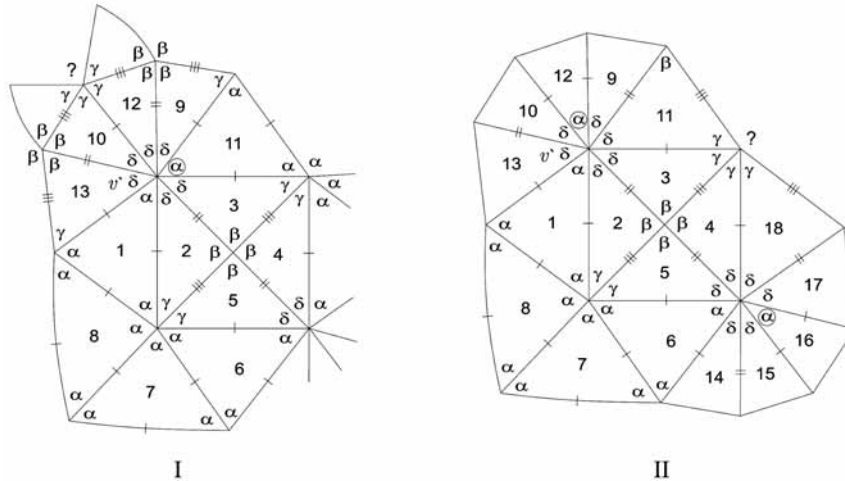


Fig. 15. – Planar representations.

2.2 If $\alpha + 2\gamma = \pi$, the angular order relation is exactly the same,

$$\frac{\pi}{6} < \delta < \gamma < \frac{\pi}{3} < \alpha.$$

The alternate angle sum at vertex v_8 containing α and δ must be

$$\alpha + \delta + \gamma = \pi \quad \text{or} \quad \alpha + 2\delta + \gamma = \pi \quad \text{or} \quad \alpha + 3\delta = \pi, \quad \text{or} \quad 2\alpha + \delta = \pi.$$

The first case is incompatible with the assumption $\alpha + 2\gamma = \pi$.

As $\gamma + \delta > \frac{\pi}{2}$ and $\alpha > \gamma$, then $\alpha + 2\delta + \gamma > \pi$ and the second case must be eliminated. The third case should be discarded, using a similar reasoning to the one made in case 2.1 under the same assumption. Suppose now that $2\alpha + \delta = \pi$. By the adjacency condition we get $\gamma \approx 56.489^\circ$, $\alpha \approx 67.022^\circ$ and $\delta \approx 45.956^\circ$.

Starting from configuration in Figure 14 we are led, according to the edge position of tile 6, to one of the configurations illustrated in Figure 16.

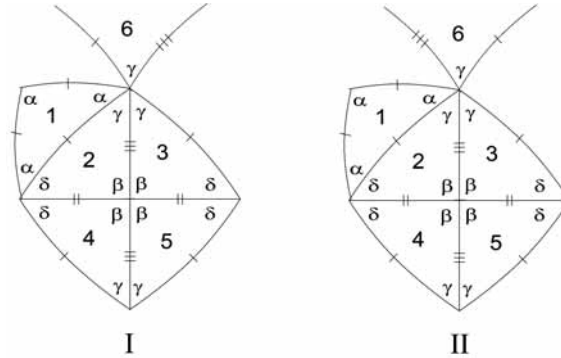


Fig. 16. – Planar representations.

Taking as starting point the configuration I, in Figure 16 we get the one in Figure 17-I, which is impossible to be expanded, since the alternate angle sums at vertex v_9 do not satisfy the angle folding relation (δ is not a submultiple of π and there are no other way of combining δ with any one of the other angles).

The other possible position for tile 6 gives rise to configuration II. However, the alternate angle sum containing α , γ and δ at vertex v_{10} do not satisfy the angle folding relation and so it is impossible to expand the configuration.

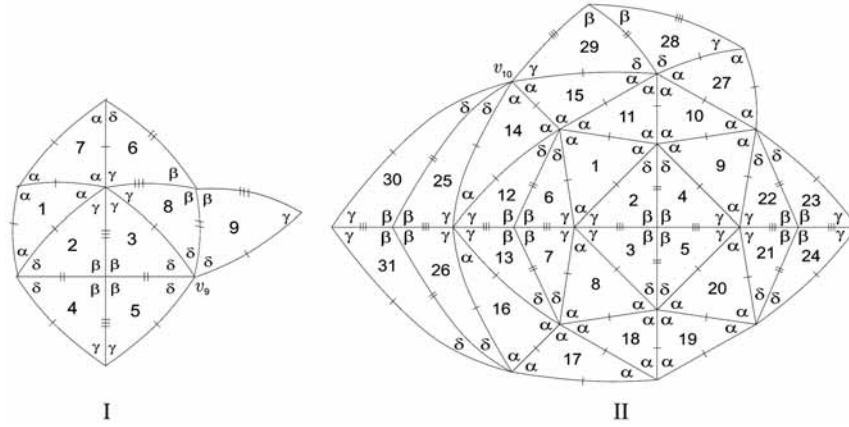


Fig. 17. – Planar representations.

2.3 Assume now that $\alpha + \gamma + t\delta = \pi, t \geq 1$. The discussion of the case $t > 2$ follows a similar reasoning to the one done for $t = 2$ and so we will focus our attention in the cases $t = 1$ and $t = 2$.

2.3.1 If $t = 1$, the configuration illustrated in Figure 18, having as a starting point the one given in Figure 14 corresponds to a particular choice of the position of tiles 6, 11 and 21. It gives rise to a tiling $\tau \in \Omega(T_1, T_2)$ composed by 24 scalene triangles and 8 equilateral triangles and will be denoted by \mathcal{F}_1^δ .

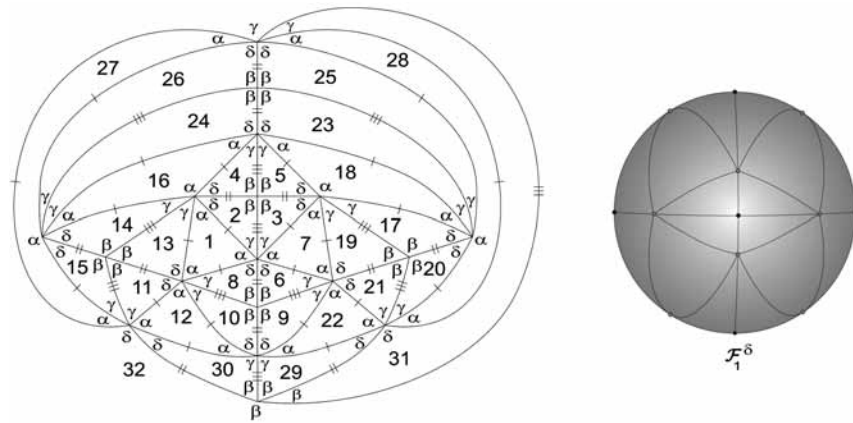


Fig. 18. – 2D and 3D representation of \mathcal{F}_1^δ .

The other possible arrangement for the length sides of tile 21 leads us to a global configuration of a tiling $\tau \in \Omega(T_1, T_2)$. This f-tiling is composed by 24 scalene triangles and 8 equilateral triangles and is denoted by \mathcal{F}_2^δ , Figure 19.

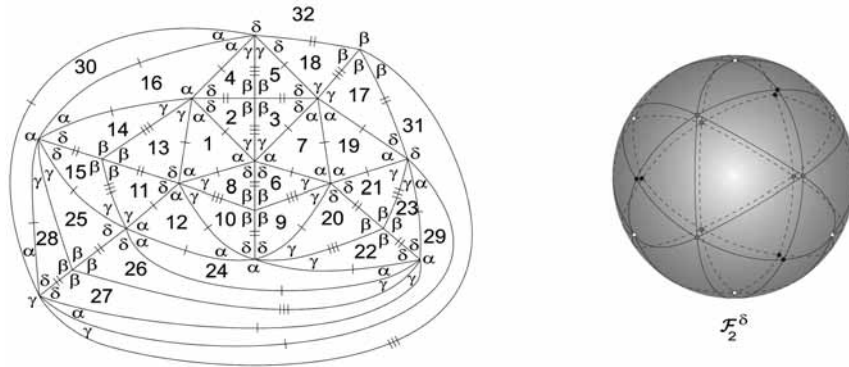


Fig. 19. – 2D and 3D representation of \mathcal{F}_2^δ .

The other position of tile 11 leads to the configuration shown in Figure 20.

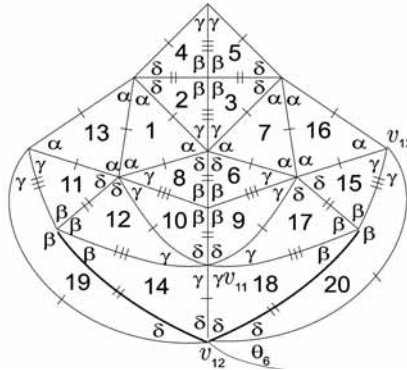


Fig. 20. – Planar representation.

Looking at vertex v_{11} , we conclude that $\gamma + \delta + \gamma = \pi$ (as $2\gamma + \delta + \rho > \pi$, for any $\rho \in \{\alpha, \gamma, \delta, \beta\}$) and so $\alpha = \gamma$. At vertex v_{12} , the angle $\theta_6 \in \{\delta, \gamma, \alpha\}$.

2.3.1.1 If $\theta_6 = \delta$, then at vertex v_{13} , we obtain the alternate angle sum $2\gamma + \alpha \leq \pi$, which is an absurd.

2.3.1.2 If $\theta_6 = \gamma$, v_{12} is a vertex of valency greater than 6, otherwise $\alpha = \gamma = \delta$. Consequently, one of the alternate angle sums is $\gamma + q\delta = \pi$, $q \geq 3$. Since $2\gamma + \delta = \pi$ and $\gamma + q\delta = \pi$ one has $\delta = \frac{\pi}{2q-1}$ $\alpha = \gamma = \frac{(q-1)\pi}{2q-1}$. By the adjacency condition 1.1, we get $\frac{1 + \cos((q-1)\delta)}{\sin((q-1)\delta)} = \frac{\cos \delta}{\sin \delta}$, that is, $\sin \delta = \sin((q-2)\delta)$. Therefore, $q = 3$ and as a result $\delta = \frac{\pi}{5}$, $\alpha = \gamma = \frac{2\pi}{5}$.

However, extending configuration in Figure 20, we are led to an absurd, since the vertex surrounded by the angular sequence $(\gamma, \gamma, \gamma, \gamma, \alpha)$ violates the angle folding relation, see below (Figure 21).

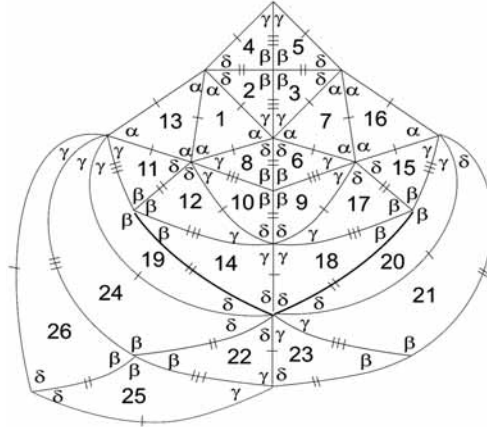


Fig. 21. – Planar representation.

2.3.1.3 If $\theta_6 = \alpha$, since $\alpha = \gamma$, we get exactly the same absurd.

The other possibility for the length sides of tile 6 permits to extend a bit more the configuration in Figure 14 and a decision on $\theta_7 \in \{\delta, \alpha\}$ must be taken (see Figure 22).

If $\theta_7 = \delta$, the configuration is the one illustrated in Figure 23-I. This configuration expands globally and we get a representation of the tiling \mathcal{F}_2^δ .

If $\theta_7 = \alpha$, we get the configuration II illustrated in Figure 23. Observe that tile 16 obliges that one of the alternate angle sums at vertex v_{14} is $2\alpha + \delta = \pi$. Adding some new cells to this configuration we get a vertex

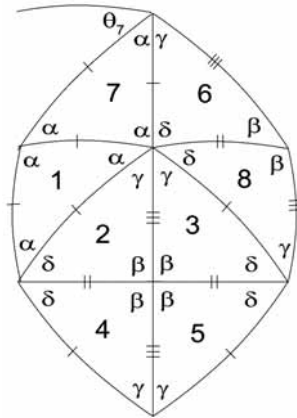


Fig. 22. – Planar representation.

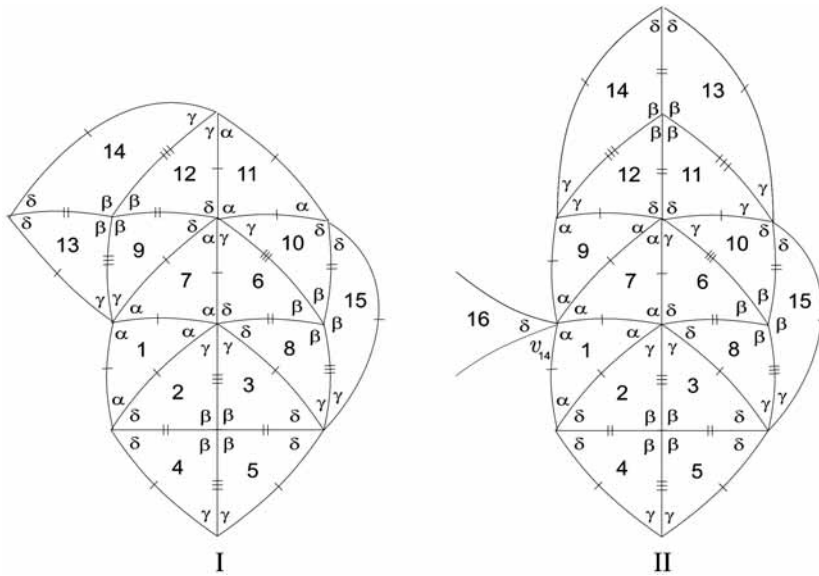


Fig. 23. – Planar representations.

surrounded by alternate angles $(\gamma, \gamma, \alpha, \gamma, \gamma)$, which is absurd (see Figure 24). Suppose now, that $\alpha + \gamma + t\delta = \pi$, for $t > 1$. Having in account that $\gamma + \delta > \frac{\pi}{2}$, then $\gamma > \alpha + (t - 2)\delta \geq \alpha$.

$$\text{Summarizing, } \delta < \frac{\pi}{6} < \frac{\pi}{3} < \alpha < \gamma < \beta = \frac{\pi}{2}.$$

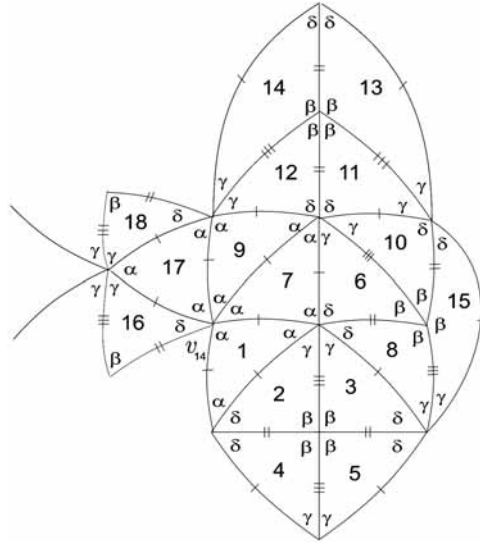


Fig. 24. – Planar representation.

2.3.2 Suppose $t = 2$.

2.3.2.1 The configuration in Figure 25 corresponds to a choice for the positions of tiles 6 and 19, with $\theta_8 \in \{\delta, \gamma, \alpha\}$.

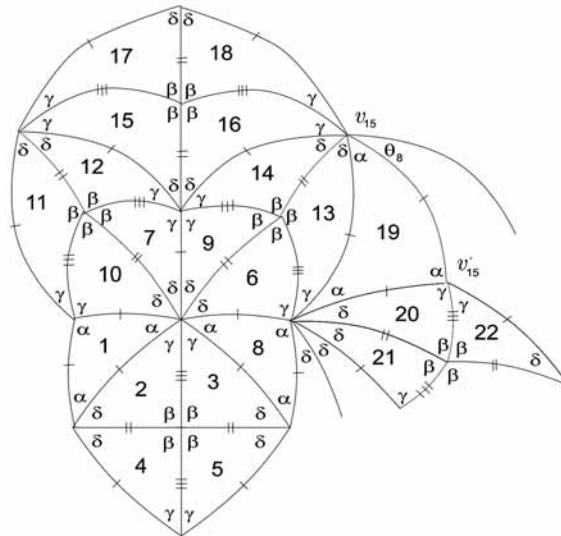


Fig. 25. – Planar representation.

If $\theta_8 = \delta$, then vertex v'_{15} is of valency 6 with alternate angle sums $2\gamma + \delta = \pi$ and $\alpha + \delta + \gamma = \pi$, contradicting our assumption.

If $\theta_8 = \gamma$, one of the alternate angle sum at vertex v_{15} is $2\gamma + \delta + \mu = \pi$, for $\mu \in \{\alpha, \delta, \gamma, \beta\}$, which is an absurd. Therefore, $\theta_8 = \alpha$. Adding some new cells to the configuration we are led to the one in Figure 26, containing a vertex surrounded by the angular sequence $(\gamma, \gamma, \alpha, \gamma, \gamma, \dots)$. Since $\gamma + \alpha + \gamma > \pi$, this configuration does not give rise to a f-tiling.

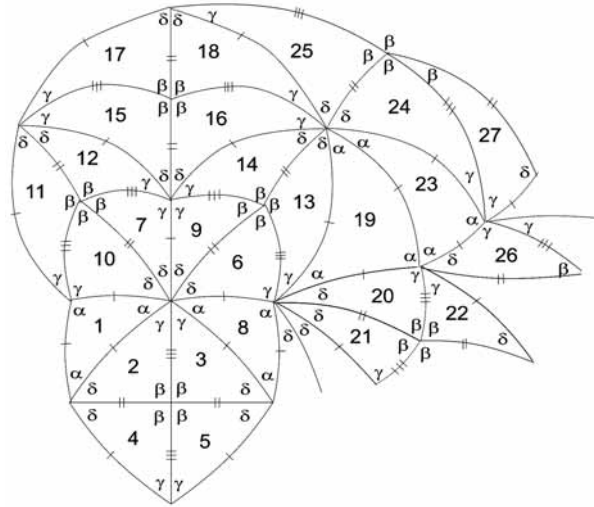


Fig. 26. – Planar representation.

2.3.2.2 If tiles 19 and 21 are, respectively, a scalene triangle and an equilateral triangle, then tile 27 is an equilateral triangle. We are led to a vertex surrounded by the angular sequence $(\gamma, \gamma, \alpha, \gamma, \gamma, \dots)$, which, as seen before, is an absurd (see Figure 27).

2.3.2.3 If tile 21 is a scalene triangle, adding some tiles to the configuration we end up to the one illustrated in Figure 28. Vertex v_{16} is surrounded in circular order by the sequence $(\gamma, \delta, \delta, \delta, \delta, \delta, \delta)$ and $\gamma + 3\delta = \pi$ implies that $\delta = \alpha > \frac{\pi}{3}$, which is an absurd and $\gamma + 4\delta = \pi$ implies that $\delta = \frac{\pi}{7}, \gamma = \frac{3\pi}{7}$ and $\alpha = \frac{2\pi}{7}$, which is also an absurd.

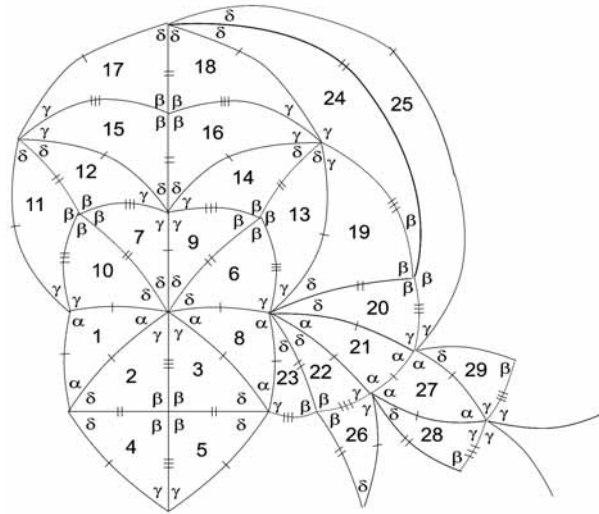


Fig. 27. – Planar representation.

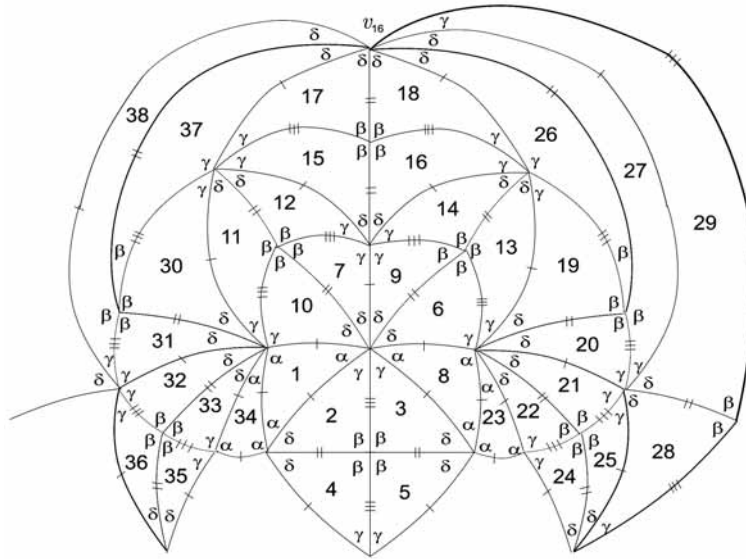


Fig. 28. – Planar representation.

2.3.2.4 Changing the order sides of tile 6 and assuming that tile 9 is a scalene triangle, we end up with configuration Figure 29, where $\theta_9 \in \{\gamma, \alpha, \delta\}$.

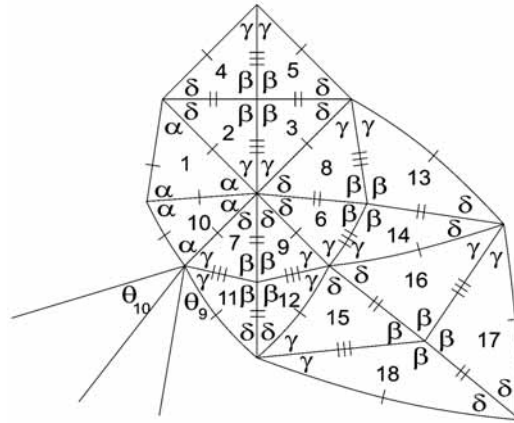


Fig. 29. – Planar representation.

If $\theta_9 = \alpha$, we are led to a configuration with a vertex surrounded by alternate angles $\gamma, \delta, \delta, \delta$, which, as seen before, is an absurd. If $\theta_9 = \gamma$, then one of the alternate angle sum at the vertex does not satisfy $\alpha + \gamma + 2\delta = \pi$. Since $\theta_9 = \delta$, then $\theta_{10} \in \{\alpha, \delta\}$. Suppose $\theta_{10} = \alpha$. Then, extending the configuration we end up in an absurd similar to the one in 2.3.2.2. Therefore, $\theta_{10} = \delta$ and the configuration is the one illustrated below (Figure 30). At vertex v_{17} , one of the alternate angle sum is $\gamma + \alpha + \gamma > \pi$, which is an absurd.

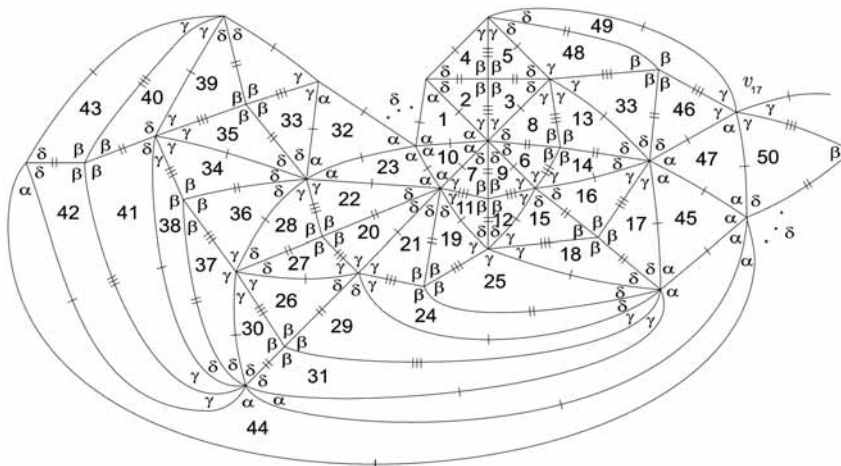


Fig. 30. – Planar representation.

2.3.2.5 Finally, if tile 9 is an equilateral triangle, in order to have, at vertices v_{18} and v_{19} , the alternate angle sum $\alpha + \gamma + 2\delta = \pi$, then $\theta_{11} = \alpha$ (see Figure 31).

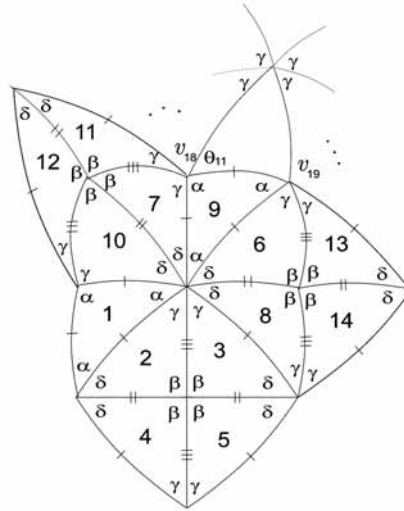


Fig. 31. – Planar representation.

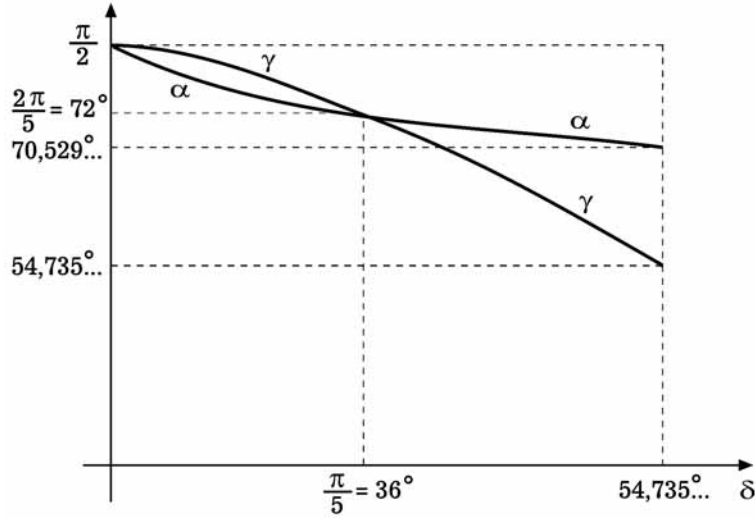
Looking at vertex surrounded by angles $(\gamma, \gamma, \alpha, \gamma, \gamma)$, we conclude that this configuration will not expand, since $2\gamma + \alpha > \pi$. \square

REMARK. – The equation (1.1) with $\beta = \frac{\pi}{2}$ and $\alpha = \pi - (\gamma + \delta)$ is writing in the form

$$(2.1) \quad \frac{-\cos(\gamma + \delta)}{1 + \cos(\gamma + \delta)} = \frac{\cos \gamma \cos \delta}{\sin \gamma \sin \delta}$$

and one the angles γ or δ is completely determined when the remaining is fixed.

In [3] it was proved that (2.1) has the solution $\delta = \gamma \approx 54.735^\circ$ (case when the triangle T_2 is isosceles). The graphic illustration in Figure 32 shows the variations of γ and $\alpha = \pi - (\gamma + \delta)$, when $\delta \in]0, 54.735^\circ[$. Therefore the f-tilings \mathcal{F}_1^δ and \mathcal{F}_2^δ represented in Figure 18 and Figure 19, respectively, are continuous families with $0 < \delta < 54.735^\circ$.


 Fig. 32. – α and γ as functions of δ .

3. Symmetry Groups

Here we present the group of symmetries of the spherical f-tilings obtained \mathcal{F}_1^δ and \mathcal{F}_2^δ . We also determine the transitivity classes of isogonality and isohedrality.

In **Table 1** it is shown a list of the dihedral f-tilings, whose prototiles are an equilateral triangle T_1 of angle α and a scalene triangle T_2 of angles δ, γ, β , ($\delta < \gamma < \beta$) in a particular way of adjacency. We have used the following notation.

- M and N are, respectively, the number of triangles congruent to T_1 and the number of triangles congruent to T_2 used in such dihedral f-tilings;
- $G(\tau)$ is the symmetry group of the f-tiling τ . We shall say that the tiles T and T' of τ are in the same *transitivity class* if the symmetry group $G(\tau)$ contains a transformation that maps T into T' . If all the tiles of τ form one transitivity class we say that τ is *tile-transitive* or *isohedral*. If there are k transitivity classes of tiles, then τ is *k-isohedral*. On the other hand, if $G(\tau)$ contains transformations that map every vertex of τ into another vertex, then we say that the vertices form one transitivity class or that τ is *isogonal*. If there are k transitivity classes of vertices, then τ is *k-*

isogonal. The numbers of isohedrality-classes and isogonality-classes for the symmetry group are denoted, respectively, by $\#$ isoh. and $\#$ isog.

With respect to tiling \mathcal{F}_1^δ the reflections on the coordinate planes generate $G(\mathcal{F}_1^\delta)$. It follows that $G(\mathcal{F}_1^\delta)$ is isomorphic to $C_2 \times C_2 \times C_2$. Now, there are 1 transitivity class of equilateral triangles and 3 transitivity classes of scalene triangles, which means that \mathcal{F}_1^δ is 4-isohedral. On the other hand, numbering the vertices of the first octant, we conclude that \mathcal{F}_1^δ is 6-isogonal.

Concerning to tiling \mathcal{F}_2^δ , the rotation of an angle $\frac{2\pi}{3}$ around the xx axis generate $G(\mathcal{F}_2^\delta)$, and so it is a cyclic group. It follows that \mathcal{F}_2^δ is 12-isohedral (2 transitivity classes of equilateral triangles and 10 transitivity classes of scalene triangles) and 6-isogonal.

- The angles δ and γ obey (2.1). Besides, $\alpha = \pi - (\gamma + \delta)$.
- $\delta_0 \approx 54.735^\circ$ and $\gamma_0 \approx 70.529^\circ$.

TABLE 1. –The Combinatorial Structure of the Dihedral F-Tilings of the Sphere by Equilateral and Scalene Triangles with adjacency of type I

f-tilings	δ	γ	α	β	M	N	$G(\tau)$	$\#$ isoh.	$\#$ isog.
\mathcal{F}_1^δ	$]0, \delta_0[$	$]\delta_0, \frac{\pi}{2}[$	$]\gamma_0, \frac{\pi}{2}[$	$\frac{\pi}{2}$	8	24	$C_2 \times C_2 \times C_2$	4	6
\mathcal{F}_2^δ	$]0, \delta_0[$	$]\delta_0, \frac{\pi}{2}[$	$]\gamma_0, \frac{\pi}{2}[$	$\frac{\pi}{2}$	8	24	C_3	12	6

REFERENCES

- [1] CATARINA P. AVELINO - ALTINO F. SANTOS, *Spherical F-Tilings by Triangles and r-Sided Regular Polygons*, $r \geq 5$, *Electronic Journal of Combinatorics*, **15** (1) (2008), #R22.
- [2] A. M. D'AZEVEDO BREDA, *A Class of Tilings of S^2* , *Geometriae Dedicata*, **44** (1992), pp. 241–253.
- [3] A. M. D'AZEVEDO BREDA - PATRÍCIA S. RIBEIRO - ALTINO F. SANTOS, *A Class of Spherical Dihedral F-Tilings*, *European Journal of Combinatorics*, **30** (1) (2009), pp. 119–132.
- [4] A. M. D'AZEVEDO BREDA - PATRÍCIA S. RIBEIRO - ALTINO F. SANTOS, *Dihedral F-Tilings of the Sphere by Equilateral and Scalene Triangles-II*, *Electronic Journal of Combinatorics*, **15** (1) (2008), #R91.
- [5] A. M. D'AZEVEDO BREDA - PATRÍCIA S. RIBEIRO - ALTINO F. SANTOS, *Dihedral F-Tilings of the Sphere by Equilateral and Scalene Triangles-III*, *Electronic Journal of Combinatorics*, **15** (1) (2008), #R147.

- [6] A. M. D'AZEVEDO BREDÁ - ALTINO F. SANTOS, *Dihedral F-Tilings of the Sphere by Spherical Triangles and Equiangular Well Centered Quadrangles*, Beiträge Algebra Geometrie, **45** (2004), pp. 441–461.
- [7] A. M. D'AZEVEDO BREDÁ - A. F. SANTOS, *Dihedral F-Tilings of the Sphere by Rhombi and Triangles*, Discrete Math. Theoretical Computer Sci., **7** (2005), pp. 123–140.
- [8] M. BERGER, *Geometry*, Volume 2, Section 18.4, Springer-Verlag, New York, 1996.
- [9] S. A. ROBERTSON, *Isometric Folding of Riemannian Manifolds*, Proc. Royal Soc. Edinb. Sect. A, **79** (1977), pp. 275–284.

Manoscritto pervenuto in redazione il 15 gennaio 2009.